High local disorder in $Tb_2Hf_2O_7$ pyrochlore oxide nanocrystals

2016 J. Phys.: Conf. Ser. 712 012113

(http://iopscience.iop.org/1742-6596/712/1/012113)

High local disorder in $Tb_2Hf_2O_7$ pyrochlore oxide nanocrystals

V A Kabanova[1], V V Popov[1], Ya V Zubavichus[2], E S Kulik[2], A A Yaroslavtsev[1,3,4], R V Chernikov[5], A P Menushenkov[1]

[1]National Research Nuclear University "MEPhI", Kashirskoe sh. 31, 115409 Moscow, Russia
[2]NRC "Kurchatov Institute", Akademika Kurhatova sq. 1, 123182 Moscow, Russia
[3]European XFEL GmbH, Albert-Einstein-Ring 19, 22761 Hamburg, Germany
[4]I. Institut für Theoretische Physik, Universität Hamburg, Jungiusstrasse 9, 20355 Hamburg, Germany
[5]DESY Photon Science, Notkestrasse 85, 22607 Hamburg, Germany

E-mail: victoria.kabanova@gmail.com

Abstract. The process of $Tb_2Hf_2O_7$ nanocrystals formation upon annealing to 1600°C was investigated by means of X-ray absorption fine structure (XAFS) spectroscopy combined with X-ray diffraction (XRD) and pair distribution function (PDF) analysis. The structure ordering and the growth of nanocrystals upon annealing were estimated independently from XRD patterns and PDF. The probable content of Tb^{4+} ions in $Tb_2Hf_2O_7$ was estimated from XANES. All studies indicate a high disorder and a large number of local structure defects in $Tb_2Hf_2O_7$ pyrochlore oxide.

1. Introduction

Double oxides of the form $Ln_2M_2O_7$ (where Ln = lanthanide, M = Ti, Zr, Hf) have a variety of potential applications as thermal barrier coatings [1], ionic conductors [2], scintillators [3], semiconductors [4] and matrices for high level nuclear wastes immobilization [5]. A number of these applications depend upon the structure of these compounds, which are able to undergo an order – disorder phase transition from pyrochlore (*Fd-3m* space group) to defect fluorite (*Fm-3m* space group) structure [6,7]. When defect fluorite structure is formed, both cations local surrounding is identical, containing 8 oxygen atoms in the cube vertices. In case of pyrochlore structure, M^{4+} oxygen surrounding changes to octahedral (CN=6), while cubic Ln^{4+} surrounding splits into 2 shorter and 6 longer Ln-O distances. Stability of pyrochlore structure is generally related to the ratio of Ln^{3+} and M^{4+} ionic radii, and is normally observed for $R_{Ln^{3+}}/R_{M^{4+}}$=1.46-1.78, while smaller values lead to defect fluorite structure formation [6,8].

However, the question concerning phase transition boundary is controversial [7-12], and the most interesting are compounds with the ratio $R_{Ln^{3+}}/R_{M^{4+}}$~1.46, in which both pyrochlore and defect fluorite structures might form depending on the synthesis conditions [13]. The aim of the current work was to study the local crystalline structure formation in one of these "boundary" compounds, $Tb_2Hf_2O_7$ ($R_{Tb^{3+}}/R_{Hf^{4+}}$=1.46), upon isothermal annealing of an amorphous precursor.

2. Experimental

The mixed Tb-Hf hydroxide was prepared by co-precipitation from $Tb(NO_3)_3 \cdot 5H_2O$ (99.99% pure), $HfOCl_2 \cdot 8H_2O$ (98+% pure) and $NH_3 \cdot H_2O$ (analytical grade). The $Tb_2Hf_2O_7$ powders were obtained by isothermal annealing of the resulting $Tb_2O_3 \cdot 2HfO_2 \cdot 10.5H_2O$ precursor at 600-1600°C for 3 h. A more detailed description of the preparation technique may be found in [14].

The powder XRD patterns were measured at beamline "Structural Material Science" of Kurchatov Synchrotron Radiation Source (Moscow, Russia) (λ=0.68886 Å, sample to detector distance 150 mm) and processed by Rietveld method. The powder XRD patterns for pair distribution function (PDF) analysis were collected at beamline P02.1 of PETRA-III storage ring (DESY, Hamburg) using high-energy photons of 59.82 keV (λ=0.207270 Å) to get a high q-range up to 21 $Å^{-1}$. PDFgetX2 [15] was used to calculate full structure factors and pair distribution functions from experimental XRD patterns. Modeling of the obtained experimental PDFs was performed using PDFgui [16].

The X-ray absorption spectra were measured at I811 beamline of MAX-lab (Lund, Sweden) and at beamline "Structural Material Science" of Kurchatov Synchrotron Radiation Source in transmission geometry above the L_3-Tb (7514 eV) and L_3-Hf (9561 eV) absorption edges at room temperature. VIPER software pack [17] was used for extraction and fitting of EXAFS-functions. Amplitudes and phases of photoelectron back scattering were calculated with FEFF code [18] using the parameters of pyrochlore structure and diffraction data. Modeling of the near-edge region of spectra was performed using XANDA software pack [19].

3. Results and discussion

XRD study has shown that isothermal annealing of X-ray amorphous mixed hydroxide at 600-700°C leads to the formation of nanocrystalline powders with the defect fluorite structure. A further annealing temperature increase leads to an increase in coherent scattering lengths and a decrease in microstrain values. Heat treatment at temperature ≥1400°C initiates nucleation and growth of nanodomains with pyrochlore-type superstructural ordering of cations inside a microcrystalline matrix with the defect fluorite structure.

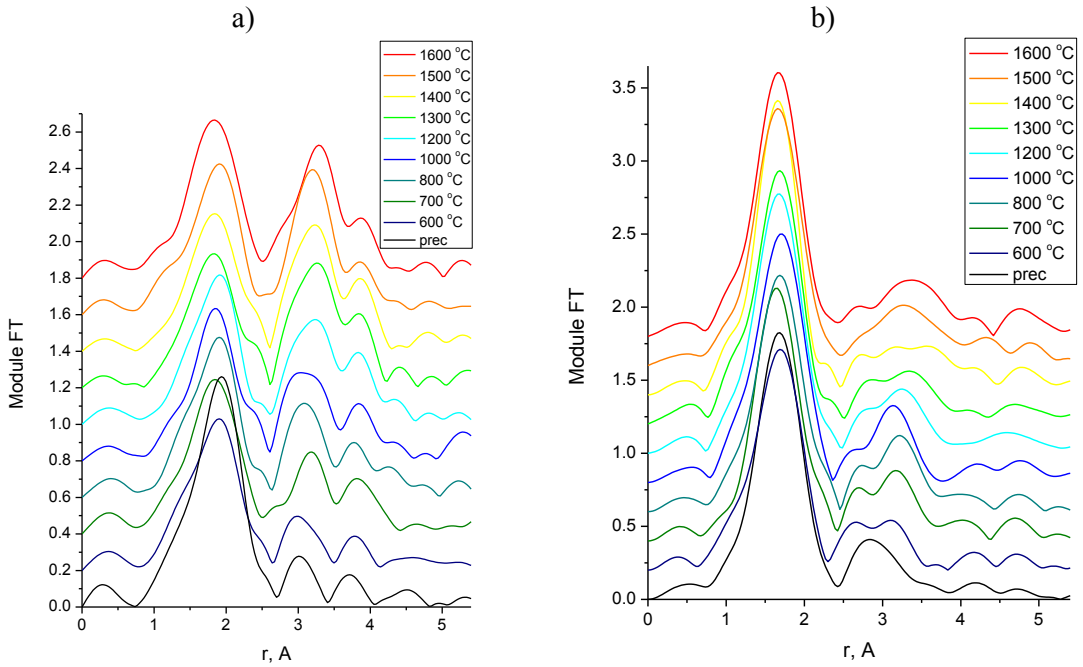

Figure 1. Fourier-Transform (FT) modules of EXAFS-functions above L_3-Tb (a) and L_3-Hf (b) edges.

According to the qualitative EXAFS analysis (figure 1), there is a slight shift of the EXAFS Fourier transform peaks corresponding to the 1st coordination shell, which indicates Tb-O and Hf-O bond

lengths contraction upon annealing. The next maxima corresponding to the metal-metal bonds change their shape and intensities, signifying the structure ordering in the course of annealing.

Modeling of EXAFS spectra was performed using both pyrochlore and defect fluorite models with fixed coordination numbers for all bonds. As a clearly pronounced non-equivalence of cations local surroundings was obvious (figure 1) and as there was a significant discrepancy of experimental data and a defect fluorite model curves, the pyrochlore model was chosen. The splitting of the 1st coordination shell Tb-O into two components was present for the samples in the whole range of investigated annealing temperatures including the precursor sample. The refined values of bond lengths and Debye-Waller factors for the 1st coordination shell are shown in figure 2. The fitting results indicate high disorder and a large number of structure defects.

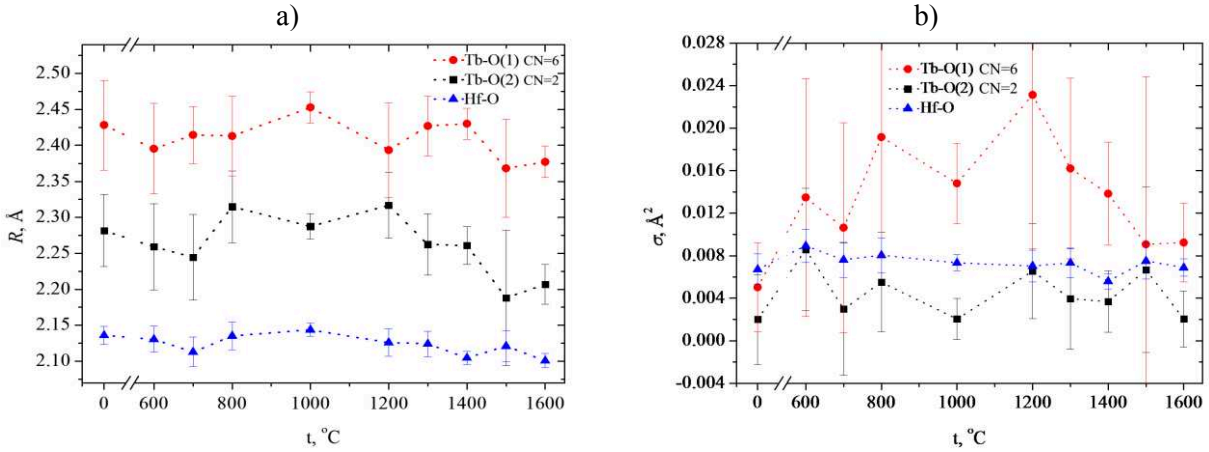

Figure 2. Bond lengths (a) and Debye-Waller factors (b) evolution with an annealing temperature increase.

It was found that X-ray absorption near edge structure (XANES) of $Tb_2Hf_2O_7$ spectra contains two contributions, which probably correspond to the Tb^{3+} and Tb^{4+} oxidation states. Tb^{4+} content was estimated by modeling of XANES spectra with two lorentzian + arctangent functions. The highest amount was found to be ~7-8% for the sample annealed at 1000°C. It was assumed that, according to the charge, Tb^{4+} ions might partially occupy the Hf^{4+} positions, which leads to an increase in structure disorder and an obstruction of the pyrochlore-type ordering.

Atomic pair distribution function (PDF) analysis shows that annealing causes an increase of interatomic distance range, in which pair correlation function G(r) maxima are still distinguishable. This corresponds to the nanocrystallites size growth upon annealing as the PDF oscillations for more calcined samples are present at longer distances. This qualitatively correlates with the XRD results for coherent-scattered regions.

Table 1. $Tb_2Hf_2O_7$ XRD and pair distribution function modeling results.

Annealing temperature	Latt. param., Å (XRD results)	Latt.param., Å (PDF analysis)	$U_{iso}(Tb^{3+}/Hf^{4+})$, Å^2
1000°C	5.21439	5.2107	0.01942
1200°C	5.2181	5.20443	0.01613
1300°C	5.22182	5.21037	0.01559
1400°C	5.22443	5.21242	0.01462
1500°C	5.22974	5.21641	0.01444
1600°C	5.23358	5.2186	0.01457

Modeling of the experimental pair distribution functions was performed using a defect fluorite model. A good convergence of experimental and refined curves was present for the long range order, but in the range of short interatomic distances a significant discrepancy was observed. This indicates

pyrochlore-type local structure of samples, while the average structure is well described by the defect fluorite model. The refined lattice parameter values demonstrate increasing dependency from an annealing temperature, which is in agreement with diffraction results (table 1). It was also found that cations anisotropic displacement parameters U_{iso} decrease upon calcination (table 1), corresponding to structure ordering.

4. Conclusion

The evolution of $Tb_2Hf_2O_7$ crystalline, local and electronic structure parameters upon annealing of initial mixed hydroxide has been studied by a complex of diffraction and absorption synchrotron methods. It has been shown that isothermal annealing of the X-ray amorphous precursor at temperatures above 600-700°C first leads to the formation of oxide nanocrystalline powders with a defect fluorite structure. Also, calcination temperature increase reveals an increase in coherent scattering lengths and a decrease in microstrain values. Heat treatment at temperature ≥1400°C initiates nucleation and growth of nanodomains with pyrochlore-type superstructural ordering of cations inside a microcrystalline fluorite matrix. Investigation of the local structure of prepared samples showed that all synthesized $Tb_2Hf_2O_7$ powders had clearly pronounced nonequivalence of the Tb^{3+} and Hf^{4+} cations local environment. It was assumed that the observed local structure disorder of $Tb_2Hf_2O_7$ samples may partially occur due to the presence of Tb^{4+} cations.

Acknowledgements

The authors thank J. Bednarcik (DESY Photon Science), R.V. Chernikov (DESY Photon Science) and S. Carlson (MAX IV lab.) for their help in experiments and the Russian Science Foundation (grant 14-22-00098) for financial support.

References

[1] Cao X Q, Vassen R and Stoever D 2004 *J. Eur. Ceram. Soc.* **24** 1-10
[2] Yamamura H, Nishino H, Kakinuma K and Nomura K 2003 *Solid State Ionics* **158** 359-65
[3] Hansel R A, Desai S K, Allison S W, Heyes A and Walker D G 2010 *J. Appl. Phys.* **107** 016101
[4] Wei F, Tu H, Wang Y, Yue S and Du J 2009 *J. Phys.: Conf. Ser.* **152** 012003
[5] Ewing R C, Weber W J and Lian J 2004 *J. Appl. Phys.* **95** 5949-71
[6] Subramanian M A, Aravamudan G and Rao G V S 1983 *Prog. Solid State Chem.* **15** 55-143
[7] Blanchard P E R, Liu S, Kennedy B J, Ling C D, Zhang Z, Avdeev M, Cowie B C C,Thomsen L and Jang L Y 2013 *J. Phys. Chem*. C. **117** 2266-73
[8] Popov V V, Menushenkov A P, Zubavichus Ya V, Yaroslastsev A A and Leshchev D S 2013 *Russ. J. Inorg. Chem.* **58** 1400-7
[9] Stanek C R 2003 Ph. D. Thesis. Imperial College. London. UK
[10] Mandal B P, Garg N and Sharma S M 2006 *J. Solid State Chem.* **179** 1990-4
[11] Zu X T, Li N and Gao F 2008 *J. Appl. Phys.* **104** 043517
[12] Popov V V, Zubavichus Ya V, Menushenkov A P, Yaroslavtsev A A, Kulik E S, Pisarev A A and Kolyshkin N A 2015 *Russ. J. Inorg. Chem.* **60** 16-22
[13] Popov V V, Zubavichus Ya V, Menushenkov A P, Yaroslavtsev A A and Kulik E S 2014 *Russ. J. Inorg. Chem.* **59** 279-85
[14] Popov V V, Zubavichus Y V, Petrunin V F, Menushenkov A P, Kashurnikova O V, Korovin S A, Chernikov R V, Yaroslavtsev A A 2011 *Glass Phys. Chem.* **37** 512-20
[15] Qiu X, Thompson J W and Billinge S J L 2004 *J. Appl. Crystal* **37** 678
[16] Farrow C L, Juhas P, Liu J W, Bryndin D, Bozin E S, Bloch J, Proffen Th and Billinge S J L 2007 *J. Phys.: Condens. Matter.* **19** 335219
[17] Klementev K V 2001 *J. Phys. D: Appl. Phys.* **34** 209
[18] Rehr J J and Albers R C 2000 *Rev. Mod. Phys. B* **72** 621-54
[19] Klementiev K V, XANES dactyloscope for Windows, freeware http://www.cells.es/old/Beamlines/CLAESS/software/xanda.html